Supporting Information

Unveiling the potential of Cu–Pd/CdS catalysts to supply and rectify electron transfer for H_2 generation from water splitting†

Ejaz Hussain[a]*, Mamoona Idrees[a], Muhammad Jalil[a], Muhammad Zeeshan Abid[a], Khalid Aljohani[b],and Khezina Rafiq[a]*

[a]Institute of Chemistry, Inorganic Materials Laboratory 52S, The Islamia University of Bahawalpur-63100, Pakistan.

[b]Department of Mechanical Engineering, College of Engineering in Al-Kharj, Prince Sattam Bin Abdulaziz University, Al-Kharj, 11942, Saudi Arabia.

Corresponding authors: Dr. Ejaz Hussain; ejaz.hussain@iub.edu.pk

Dr. Khezina Rafiq; khezina.rafiq@iub.eu.pk

Chemicals

In this work, all chemicals used were of high purity. Cadmium nitrate (Sigma-Aldrich 98% pure CAS Number 10022-68-1), sodium sulfide (Sigma-Aldrich 98% pure CAS Number 1313-84-4), sodium borohydride (Sigma-Aldrich 98% pure CAS Number 16940-66-2), copper nitrate (Merck CAS Number 19004-19-4), Ethanol (CH_3CH_2OH) Sigma (95.00% CAS#64-17-5), and Distilled water (99.9% was purchase from PIAS Pakistan).

Characterization

The X-ray diffraction (XRD) patterns were obtained using a Bruker D2-phaser equipped with a LYNXEYE XE-T detector (220 V/50 Hz). A Cu Kα radiation source with a wavelength of 1.5418 Å was employed for the XRD analysis. The 40 kV and 40 mA voltages were used for the X-ray generation. 2θ scanning range was of 10° to 80° with a step size of 0.05° and a scan rate of 2° min^{-1}. Raman spectrum were obtained using the argon-laser equipped Micro Raman Renishaw spectrometer. ATR mode on a Bruker Alpha Platinum instrument with a spectral range of 4000–400 cm^{-1} was utilized to perform the FTIR characterizations. A UV-VIS spectrometer (V-550i RM; JASCO) was used to analyze the optical characteristics of the Pd/r-TiO2 samples. The results of scanning electron microscopy (SEM) at various scales were obtained using a FEI-Nova NanoSEM-450 electron microscope equipped with an EDX accessory. The JEM-2021 plus LaB6 TEM was utilized to acquire TEM images for additional structural characterizations, with the aim of analyzing impurities, structural flaws in semiconductors, and crystal structure. The ESCALAB QXI X-Ray photoelectron spectrometer is utilized for XPS measurements. The oxidation state of the deposited Pd and other elements of catalysts were assessed by X-ray photoelectron spectroscopy (XPS; ESCALAB 240X; Thermo Fisher Scientific) at 24W with monochromatic Al K excitation. With a 274.9 eV bonding energy, the found spectra were calibrated to the C1s core level. AFM analysis was performed with PARKIN instruments, to determine the mechanical characteristics and location of the loaded metals on the photocatalysts surface. Thermo Fisher Axia Chemi SEM was used to obtain the SEM images.

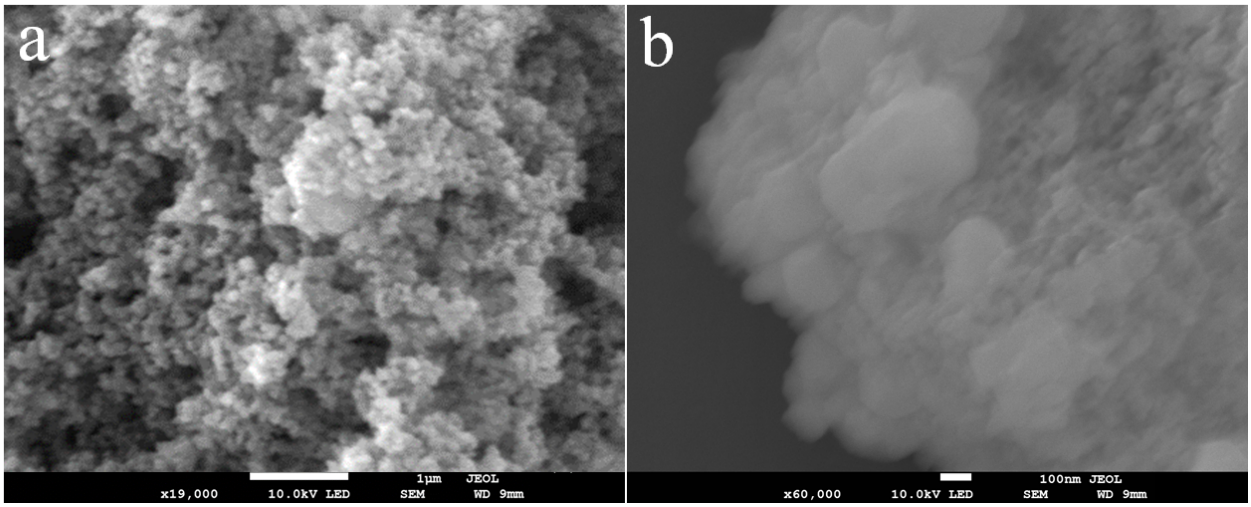

Figure S1: SEM results of used Cu–Pd/CdS catalysts at **a)** 1 µm & **b)** 100 nm.

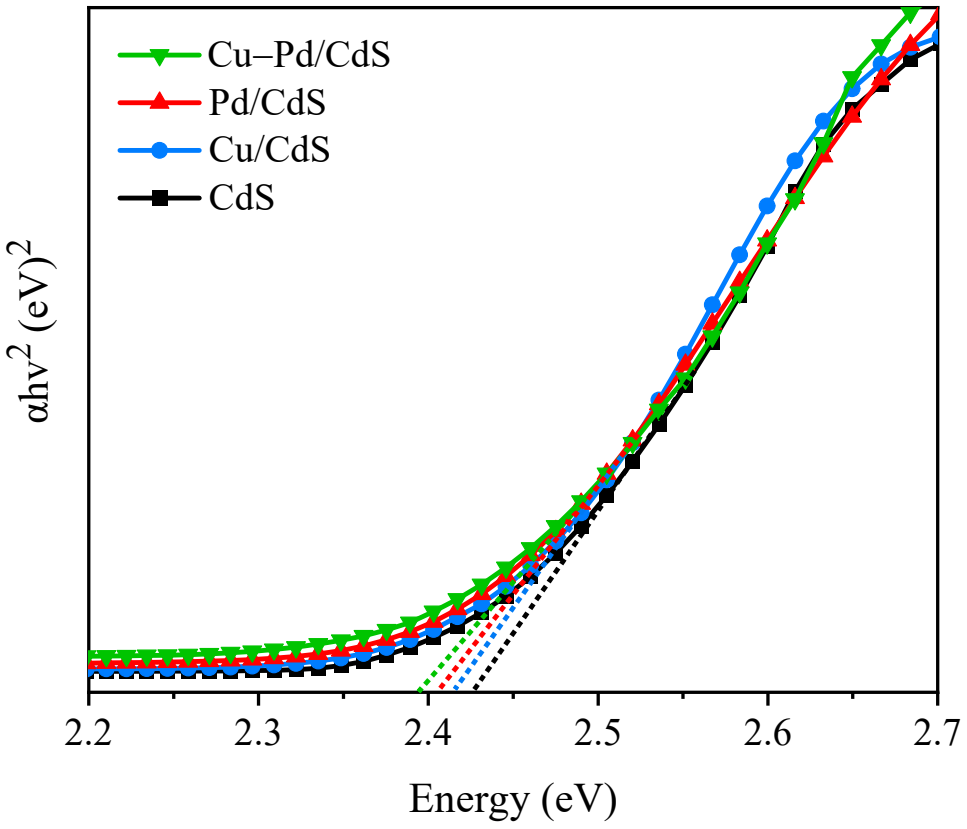

Figure S2: Bandgap energy via Tauc plot method of CdS, Cu/CdS, Pd/CdS, Cu–Pd/CdS catalysts.

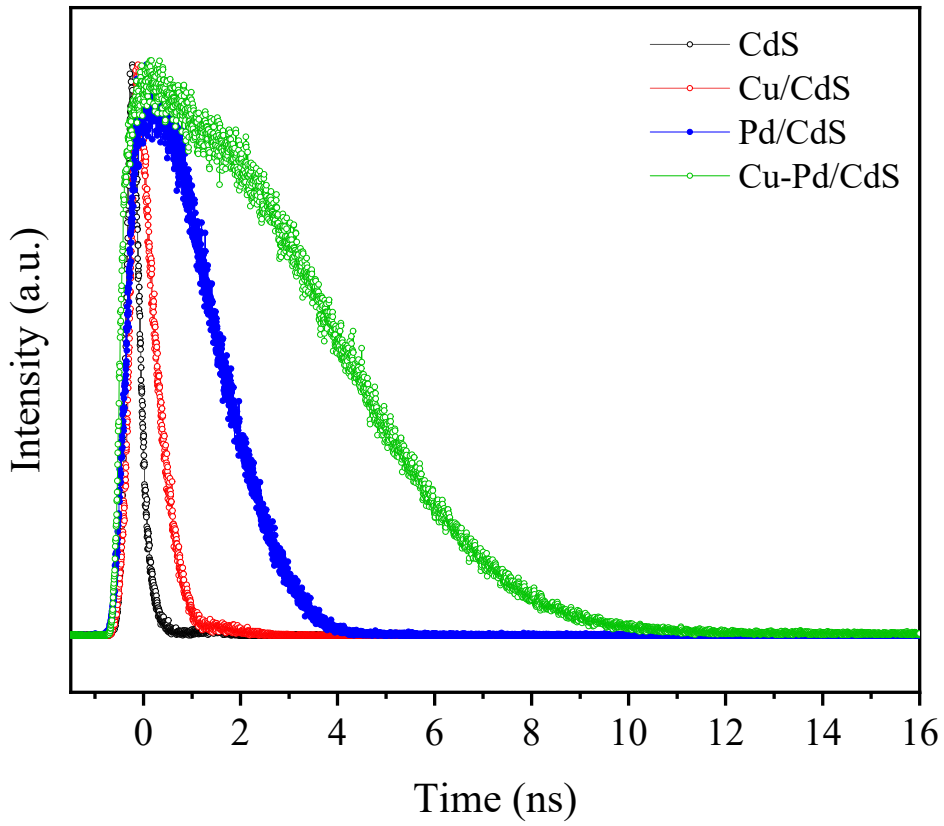

Figure S3: TRPL results of CdS, Cu/CdS, Pd/CdS, and Cu–Pd/CdS.

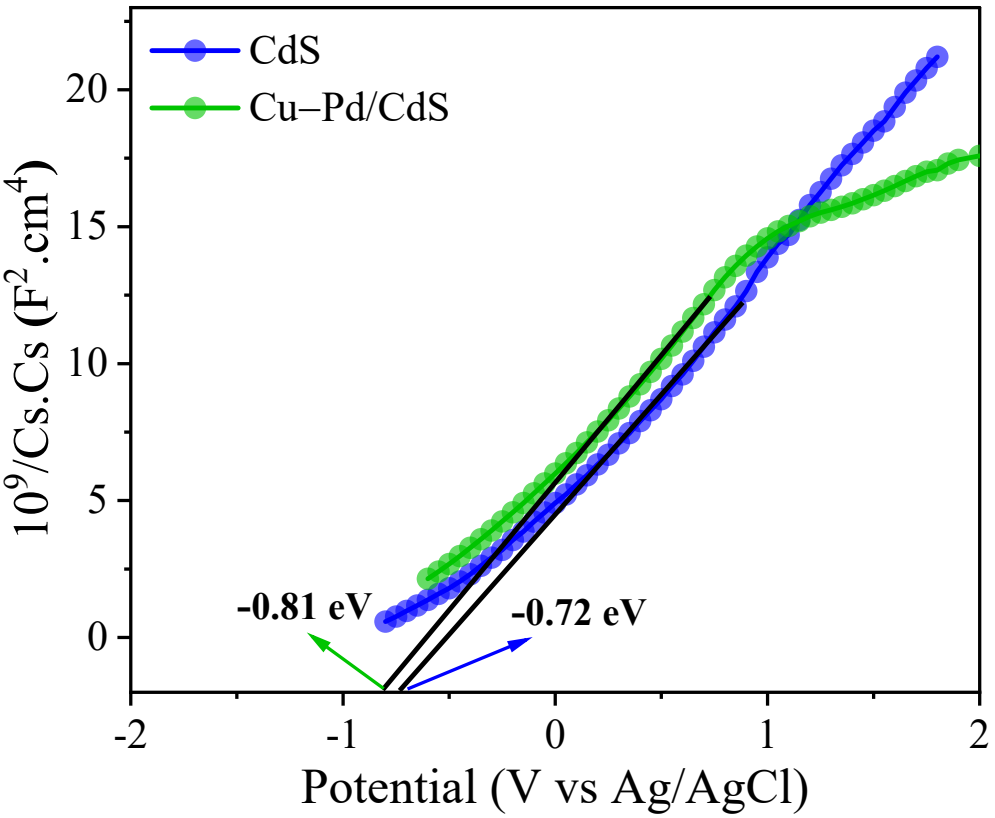

Figure S4: Mott-Schottky plot of CdS and Cu–Pd/CdS catalysts.

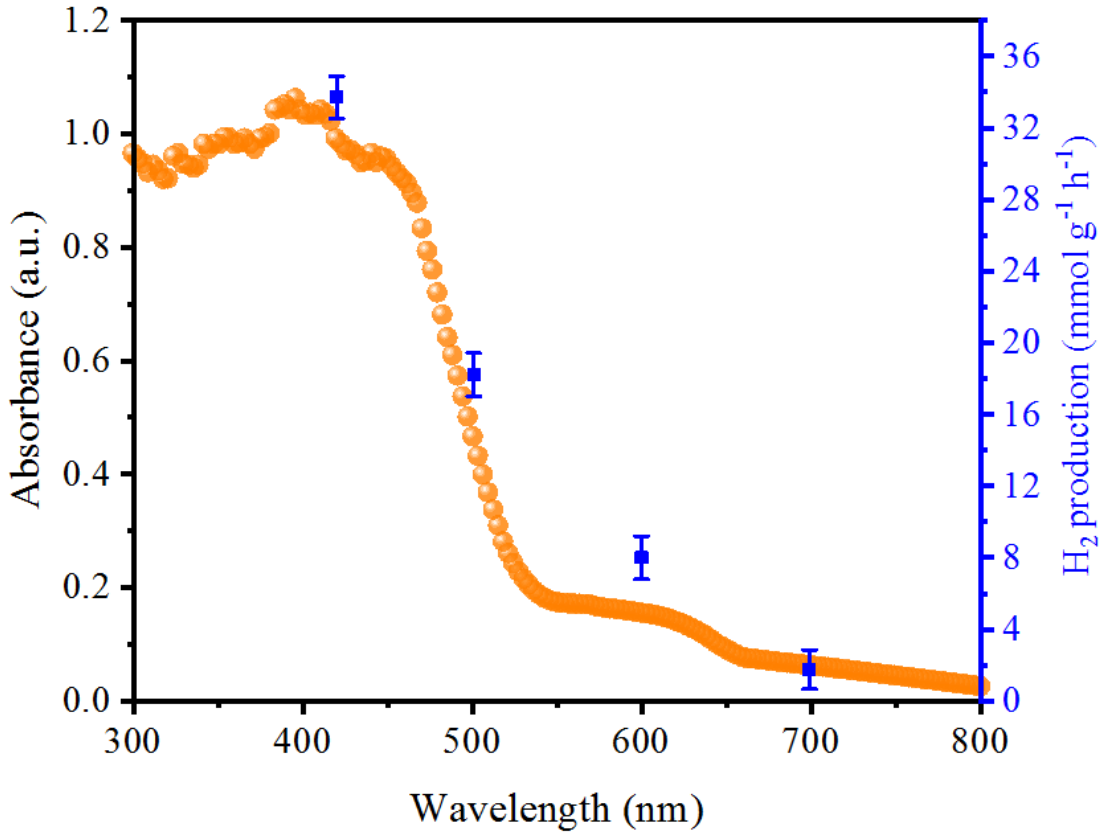

Figure S5: Wavelength dependent activities to confirm the SPR effect of Cu/Pd cocatalysts.

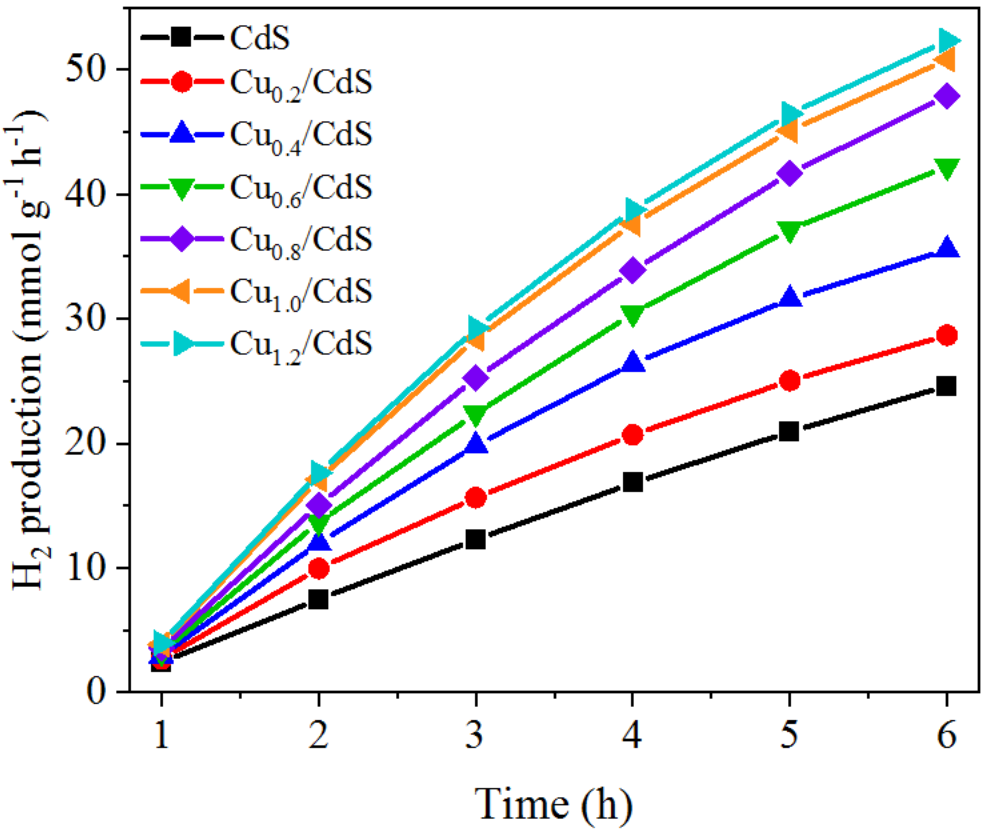

Figure S6: Optimization of % Cu at the CdS catalysts.

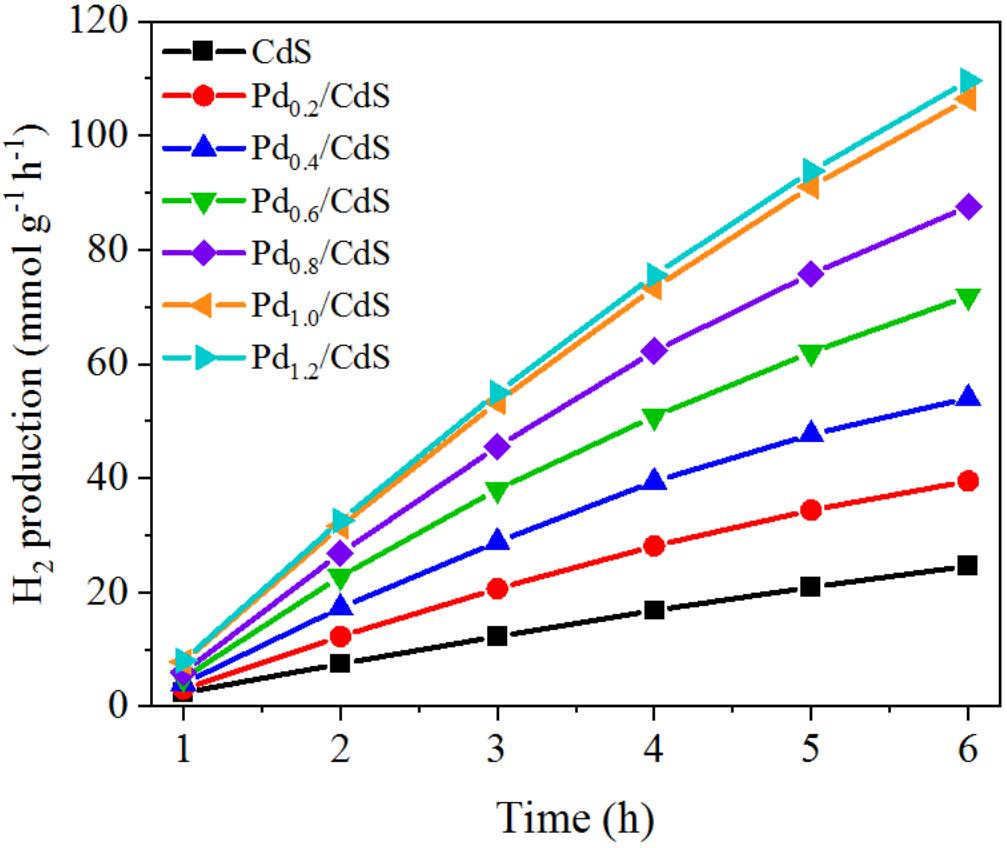

Figure S7: Optimization of % Pd at the CdS catalysts.

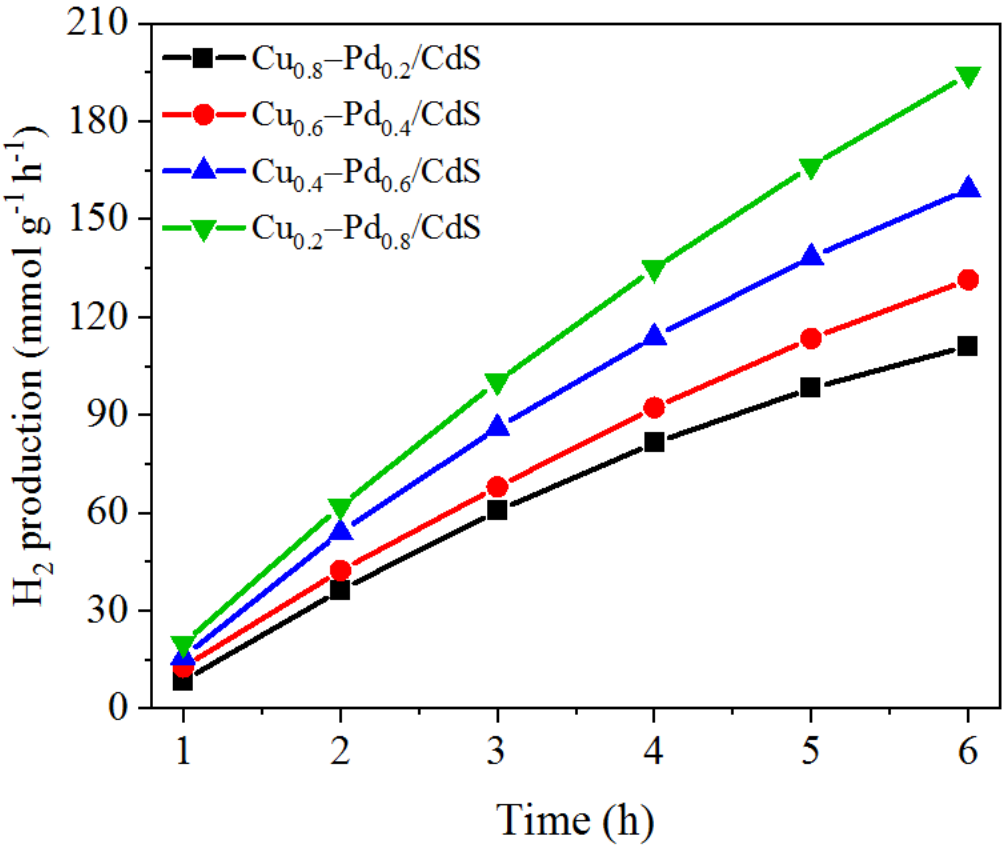

Figure S8: H_2 production values of various Cu to Pd ratios i.e., $Cu_{0.8}$–$Pd_{0.2}$/CdS, $Cu_{0.6}$–$Pd_{0.4}$/CdS, $Cu_{0.4}$–$Pd_{0.6}$/CdS, and $Cu_{0.2}$–$Pd_{0.8}$/CdS.

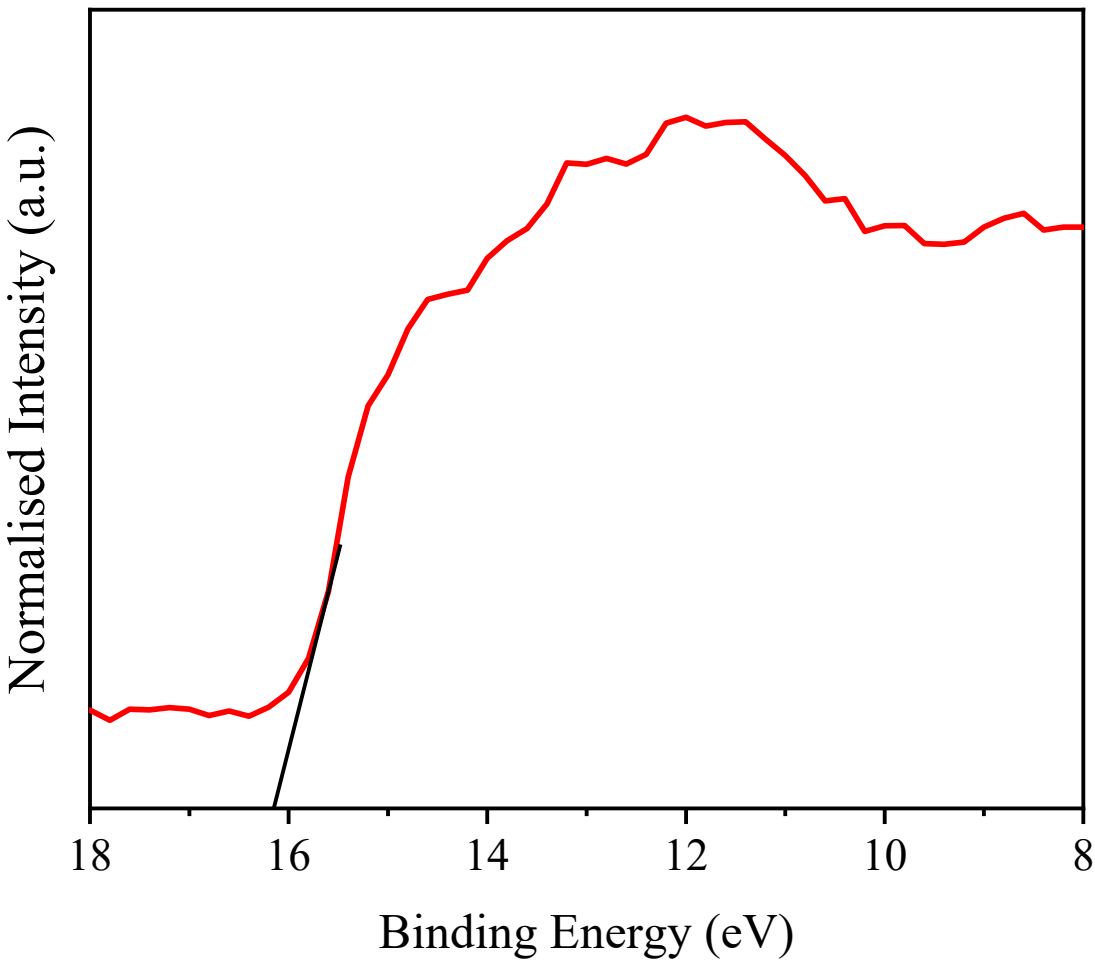

Figure S9: The secondary electron cutoff region of CdS by utilizing UPS**.**

Table S2: Data for the effect of pH.

pH	H_2 (mmol g^{-1} h^{-1})
2	8.45
4	13.45
6	19.67
8	28.65
10	33.10
12	24.65

Table S3: Data for the effect of temperature.

Temperature (°C)	H_2 (mmol g^{-1} h^{-1})
15	15.43
25	18.89
35	22.03
45	29.32
55	33.17
65	28.76

Table S4: Data for the effect of catalyst dose.

Catalyst Dose (mg)	H_2 (mmol g^{-1} h^{-1})
2	12.34
3	20.78
4	23.19
5	33.19
6	33.94
7	32.25

Table S5: Data for the effect of light intensity.

Intensity of light (W/m^2)	H_2 mmol g^{-1} h^{-1}
50	8.54
150	14.67
250	19.58
350	25.98
450	29.67
550	33.14
650	33.46

References

1. Yu, W., et al., *Superb all-pH hydrogen evolution performances powered by ultralow Pt-decorated hierarchical Ni-Mo porous microcolumns.* Advanced Functional Materials, 2023. **33**(4): p. 2210855.
2. Quyyum, U., et al., *Tunable sulphur doping in CuFe 2 O 4 for the efficient removal of arsenic through arsenomolybdate complex adsorption: kinetics, isothermal and mechanistic studies.* Environmental Science: Water Research & Technology, 2023. **9**(4): p. 1147-1160.
3. Yu, J., et al., *Synthesis of carbon-doped KNbO3 photocatalyst with excellent performance for photocatalytic hydrogen production.* Solar Energy Materials and Solar Cells, 2018. **179**: p. 45-56.
4. Xu, H.-Y., et al., *New insights into the photocatalytic mechanism of pristine ZnO nanocrystals: From experiments to DFT calculations.* Applied Surface Science, 2023. **614**: p. 156225.
5. Setiani, P., et al., *Mechanisms and kinetic model of hydrogen production in the hydrothermal treatment of waste aluminum.* Materials for Renewable and Sustainable Energy, 2018. **7**: p. 1-13.
6. Fujita, S.-i., et al., *Photocatalytic hydrogen production from aqueous glycerol solution using NiO/TiO2 catalysts: Effects of preparation and reaction conditions.* Applied Catalysis B: Environmental, 2016. **181**: p. 818-824.
7. Kampouri, S. and K.C. Stylianou, *Dual-functional photocatalysis for simultaneous hydrogen production and oxidation of organic substances.* ACS Catalysis, 2019. **9**(5): p. 4247-4270.
8. Gupta, N. and B. Pal, *Core–shell structure of metal loaded CdS–SiO2 hybrid nanocomposites for complete photomineralization of methyl orange by visible light.* Journal of Molecular Catalysis A: Chemical, 2014. **391**: p. 158-167.
9. Jiang, C., et al., *Photoelectrochemical devices for solar water splitting–materials and challenges.* Chemical Society Reviews, 2017. **46**(15): p. 4645-4660.
10. Rahman, M.Z., K. Davey, and C.B. Mullins, *Tuning the intrinsic properties of carbon nitride for high quantum yield photocatalytic hydrogen production.* Advanced Science, 2018. **5**(10): p. 1800820.